Polímeros
ISSN 1678-5169 (Online)

https://doi.org/10.1590/0104-1428.20240072

Thermal behavior of NBR vulcanizates activated with plant-extract-derived magnesium oxide[a]

Arianne Aparecida da Silva[1]*, Ana Maria Furtado de Sousa[1], Cristina Russi Guimarães Furtado[1] and Nakédia M. F. Carvalho[1]

[1]Instituto de Química, Universidade do Estado do Rio de Janeiro – UERJ, Rio de Janeiro, RJ, Brasil
**ariannesilvado20201@ppgq.uerj.br*

*[a]This paper has been partially presented at the 17th Brazilian Polymer Congress,
held in Joinville, SC, 29/Oct - 02/Nov/2023*

Abstract

This study compares the thermal degradation and aging resistance of NBR compounds activated with ZnO or MgO-green synthesized with the assistance of *Camellia sinensis* extract. Thermal degradation was studied using the Flynn-Wall-Ozawa method. Aging resistance was investigated by the changes in crosslink density and mechanical properties before and after the samples are exposed in a forced-air oven at 100 °C/72 h. The activation energies for NBR compounds with MgO-green and ZnO are, respectively, 220 kJ mol^{-1} and 700–200 kJ mol^{-1}. After oxidative-thermal aging, the crosslink density of NBR compounds goes up by 24% with MgO-green and 120% with ZnO. Consequently, the changes in hardness and tensile properties of the NBR with MgO-green are more subtle than those observed with ZnO. Based on Fisher's minimum significant difference procedure, the data analysis shows that MgO-green can be used instead of ZnO as an activator in the vulcanization of NBR.

Keywords: *activator, green magnesium oxide, NBR, thermal behavior, zinc oxide.*

How to cite: Silva, A. A., Sousa, A. M. F., Furtado, C. R. G., & Carvalho, N. M. F. (2025). Thermal behavior of NBR vulcanizates activated with plant-extract-derived magnesium oxide. *Polímeros: Ciência e Tecnologia*, *35*(1), e20250011. https://doi.org/10.1590/0104-1428.20240072

1. Introduction

Nitrile rubber (NBR) is a synthetic elastomer with excellent resistance to oil and nonpolar solvents. NBR is used extensively in the automotive, aerospace, chemical, and petrochemical industries, for instance for sealing purposes[1-4]. To produce technical goods, rubber must undergo vulcanization to form a three-dimensional network. The vulcanization system in rubber formulations is complex and consists of a combination of cure agents, accelerators, and activators, with ZnO being the most employed activator[5]. Nevertheless, the use of ZnO in rubber has faced opposition due to its potential toxicity, particularly in aquatic environments[6]. Therefore, research efforts aimed that replacing ZnO with alternative oxides can contribute to solving this problem[7-9].

Many potential alternative materials were investigated for reducing or replacing the ZnO content in rubber formulations, including zinc(II) complexes[10], zinc-based activators incorporated into porous materials like Zn-clay or supported on a substrate[11,12], and environmentally friendly activators[7,13,14]. Additionally, studies are conducted to evaluate the substitution of ZnO with MgO in natural rubber and nitrile rubber to mitigate the associated toxicity of the rubber compositions[9,15,16].

MgO is a metallic oxide with a well-known crystalline phases, regular structure, ionic nature and basic properties. It has interesting characteristics and a wide range of uses[17,18]. In our previous paper[9], we showed that the use of MgO produced by a green synthesis with the assistance of *Camellia sinensis* extract (also referred to as MgO-green) has the potential to replace ZnO in equivalent amounts in phr, mainly demonstrating convincing mechanical properties and higher cross-linking density. In the formulations with MgO-green compared to the formulations with ZnO, shorter initial vulcanization time, higher cross-link density, and excellent stress relaxation values were observed in the rheometric properties. However, further research must be conducted to establish the viability of replacing ZnO with MgO-green in NBR compounds.

Thermal properties are usually assessed using thermogravimetric analysis, which can provide valuable information about the decomposition kinetics of materials using an appropriate test method[19]. Isothermal (constant temperature) and/or non-isothermal (constant heating rate) methods have been reported for calculating kinetic parameters such as apparent activation energy (E_a), pre-exponential factor (A), reaction order (n), and rate constant (k)[20]. A widely used method is the Flynn–Wall–Ozawa integral isoconversional known as a model-free approach method, which allows the calculation of the activation energy using the Doyle approximation of the exponential integral[21].

Thermal aging plays a crucial role in materials research. Shuhaimi et al.[22] studied how the efficient (EV), semi-efficient (SEV), and conventional (CV) vulcanization systems, in the presence of natural antioxidants, play a key role in the thermal degradation of natural rubber (NR) compounds. Mechanical tests including tensile and tear essays, as well as cross-link density measurements, were conducted both before and after aging. Thermal aging analysis results are influenced by variations in the vulcanization system. Sun et al.[23] studied the activation energy for thermal air degradation of hydrogenated nitrile butadiene rubber (HNBR) filled with carbon black. The authors stated that the energy barrier for the degradation of the molecular chains of HNBR under air atmosphere increases because of the high energy of carbon-carbon single bonds. Zhang et al.[24] investigated the thermal degradation of HNBR stated that the filling with sodium methacrylate decreases the diffusion rate of the decomposition products, resulting in enhancement of the thermal stability of the composites. Furthermore, elevating the sodium methacrylate content could improve the activation energy of the composites.

Motivated by developing a sustainable rubber formulation and showing the viability of replacing ZnO with MgO-green in NBR compounds, this study aims to compare the thermal behavior of NBR/carbon black composites, activated with equal amounts in phr of ZnO or MgO-green. To address this point, we used the Flynn-Wall-Ozawa integral isoconversional method and the thermal-oxidative aging method to investigate the NBR compounds activated with ZnO or MgO-green, and compare their activation energy for degradation, and changes in crosslink density, Shore A hardness, and tensile properties.

2. Materials and Methods

2.1 Materials – Green Synthesis

Magnesium acetate tetrahydrate ($Mg(CH_3COO)_2.4H_2O$) were purchased from Neon Comercial Ltda. Dehydrated leaves of *Camellia Sinensis* (green tea) were obtained from Midori Indústria de Chá Ltda. Acetone and isopropyl alcohol was acquired from Sigma-Aldrich and Tedia Company, respectively. The synthesis protocol and characterization of MgO-green are described in Silva et al.[9].

2.2 Materials - Rubber composite

NBR N-615 (33% acrylonitrile), carbon black N330, sulfur (S), ZnO, stearic acid, *N*-tert-butyl-2-benzothiazole-sulfenamide (TBBS) were donated by Nitriflex S.A. Indústria e Comércio.

2.3 Preparation of NBR/Carbon black composites

Table 1 shows the NBR formulations (based on ASTM D3187). The compounds were prepared in a two-roll mixing mill (Luxor, model BML 150) based on the ASTM D3187 standard. Rubber Process Analyzer 2000 (Alpha Technologies) was used to determine the t_{90} values of all rubber composites at 160 °C in accordance with ASTM D5289. Rubber sheets (150 × 150 × 2mm) were vulcanized in a hydraulic press at 18 MPa of pressure, 160 °C of temperature, and t_{90} time. The experimental code used was NBR-X, where X is ZnO or MgO-green.

Table 1. NBR formulation (amount in phr) (Based on ASTM D3187).

Component	NBR-ZnO	NBR-MgO-green
NBR	100	100
Carbon black N330	40	40
Sulfur	1.5	1.5
ZnO	3	-
MgO-green (82.4% of purity)	-	3.6
Stearic acid	1	1
TBBS*	0.7	0.7

*N-tert-butyl-2-benzothiazole-sulfenamide.

2.4 Flynn-Wall-Ozawa integral isoconversional method

The pyrolysis of NBR/carbon black composites was carried out in a thermogravimetric analyzer (Q50, TA Instruments) with a scanning temperature from 25 to 600 °C and a heating rate of 5, 10, or 30 °C/min under nitrogen atmosphere. The activation energy of vulcanizate decomposition was computed using Equation 1 based on the Flynn-Wall-Ozawa method[21] outlined in ASTM E1641.

$$E_a = \left(\frac{-R}{b}\right)\frac{d\ln\beta}{d\left(\frac{1}{T}\right)} \tag{1}$$

wherein E_a is the estimated activation energy, R is the universal gas constant, b is the constant assuming $n = 1$, β is the heating rate (°C/min), and T is the temperature of weight loss (°C). The E_a can be determined using the slope between lnß and 1/T at a constant weight loss. Given that the goal of our study is to investigate the impact of cross-linking on pyrolysis, this analysis focused only on the beginning of the rubber degradation. The specified weight loss values used were 0.5, 0.6, 0.7, 0.8, 0.9, 1.0, 5.0, and 20 wt%.

2.5 Thermal-oxidative aging

The relative properties of the NBR/Carbon black composites were investigated by comparing the changes in crosslink density[25], Shore A hardness (ASTM D2240), and tensile properties (ASTM D412), before and after thermal aging in the presence of air. The test specimens were exposed in a forced-air oven at 100 °C for 72 h, according to ASTM D573.

2.6 Cross-link density

The cross-link density was determined based on solvent swelling measurements using the Flory-Rehner equation[25] (Equation 2).

$$\left[X\right] = -\frac{\left[\ln\left(1-v_r\right)+v_r+\chi v_r^2\right]}{V_0\left(v_r^{\frac{1}{3}}-\frac{v_r}{2}\right)} \tag{2}$$

wherein *[X]* is the cross-link density; v_R is the volume fraction of rubber in a swollen vulcanized sample in equilibrium; V_0 is the molar volume of the solvent (acetone: 73.4 cm^3 $g\ mol^{-1}$); χ is the interaction parameter between the solvent and the elastomer[26]. In this determination, the volume of carbon black, zinc and magnesium oxides was discounted in the value of v_R.

2.7 Mechanical property

Shore A hardness was measured using a Parabor hardness meter in accordance with ASTM D2240. Tensile tests were conducted on EMIC DL2000 according to ASTM D412. Five Type C dumbbell specimens were used, and the rate of grip separation was set at 500 mm min^{-1}.

3. Results and Discussion

3.1 Thermal degradation

Figure 1 shows the thermogravimetric curves for NBR-ZnO and NBR-MgO-green at a heating rate of 10 °C min^{-1}. These curves show the weight loss and first derivative of weight loss as a function of temperature, or DTG. Figure 2 shows the only the superposition of weight loss versus temperature curves for NBR-ZnO and NBR-MgO-green at heating rates of 5, 10, and 30 °C min^{-1}. As expected, the TGA curves shift to higher temperatures as heating rates increase.

According to Figures 1 and 2, although the curves have similar profiles, it is clear that the NBR-ZnO starts to lose mass before the NBR-MgO-green. The temperature at which a mass loss of 5% (T5%) occurs for the NBR-MgO-green is 12 °C higher than the T5% for the NBR-ZnO (Figure 1). Roy et al.[7] observed the same behavior for natural rubber vulcanized with MgO in comparison to ZnO. Furthermore, at a heating rate of 10 °C min^{-1}, the NBR-ZnO and NBR-MgO-green exhibit weight losses of 3.0 and 1.5%, respectively, between 150 and 300 °C (Figure 1). The temperature corresponding to the maximum degradation rate (maximum peak in DTG curves, T_{max}, Figure 1) is similar to the two NBR compounds since the difference between the two NBR compounds is 4 °C. The T_{max} values shown in Figure 1 are in line with the findings of Lee et al.[27], who reported a temperature of 456 °C for NBR (34% of acrylonitrile) compounds that were filled with 55 phr carbon black and activated with 5 phr of zinc oxide.

The finding about the difference in initial thermal degradation behavior of NBR-MgO-green and NBR-ZnO is particularly interesting, given that the only difference between these two samples is the type of oxide used as activator. A possible reason for this behavior is that ZnO and MgO drive the vulcanization processes differently, resulting in the formation of different types of chemical links and/or by-products, and consequently, the activation energies required to start the degradation of NBR composite would be different. So, to investigate the hypothesis further, a pyrolysis kinetic study is conducted utilizing the Flynn-Wall-Ozawa model (Equation 1), which employs a model-free kinetic isoconversional approach[28,29].

The investigation of the pyrolysis kinetics for NBR-ZnO and NBR-MgO-green involves plotting the ln (β) against 1/T graphs for weight losses in the early stages of degradation (0.5, 0.6, 0.7, 0.8, 0.9, 1.0, 5.0, and 20 wt%), as shown in Figure 3. The apparent activation energy (E_a) at a specific conversion can be derived from the slop ln (β) against 1/T. The results shown in Table 2 demonstrate the very strong correlation coefficient, showing that the model describes the experimental data properly. Figure 4 shows the comparison of E_a values for the two composites.

The E_a values for NBR-MgO-green range around 220 kJ/mol during the early stages of degradation, whereas E_a values for NBR-ZnO tend to decrease as the conversion proceeds from 0.5 to 5%wt. Furthermore, NBR-ZnO has greater E_a values than NBR-MgO-green, with the exception of 5 and 20%wt, when they have comparable E_a values. Liu et al.[30] said that the rubber pyrolysis initiates by the breakdown of side or end chains and defect structures, which required intense energy to be activated. Given that the rubber is the same in both composites, the differences in E_a in the early stages of pyrolysis (0.5 – 1.0%wt.) can be attributed to the types of crosslinks or defects presents in the network; thus, there is evidence that ZnO and MgO affect the products of the vulcanization reaction in different ways, confirming the

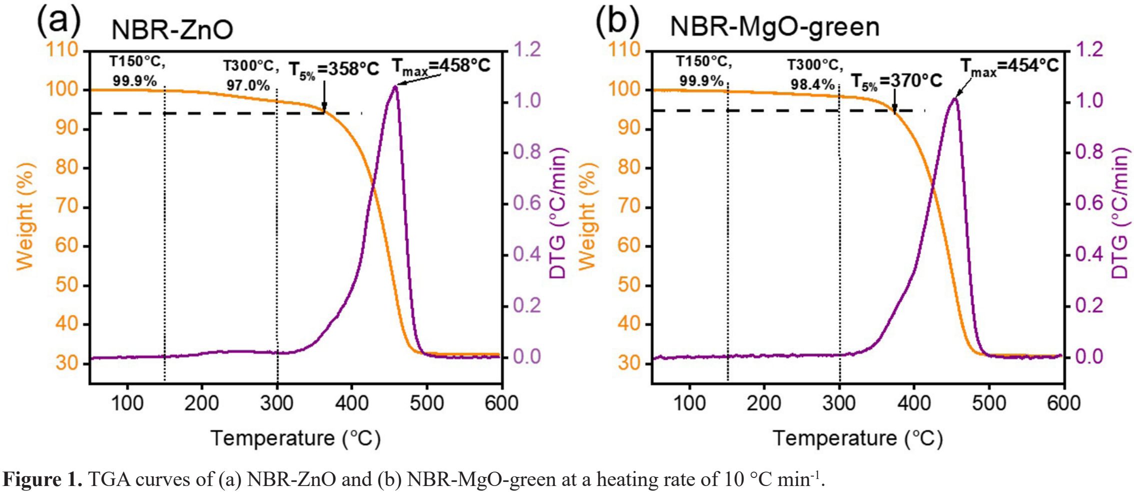

Figure 1. TGA curves of (a) NBR-ZnO and (b) NBR-MgO-green at a heating rate of 10 °C min^{-1}.

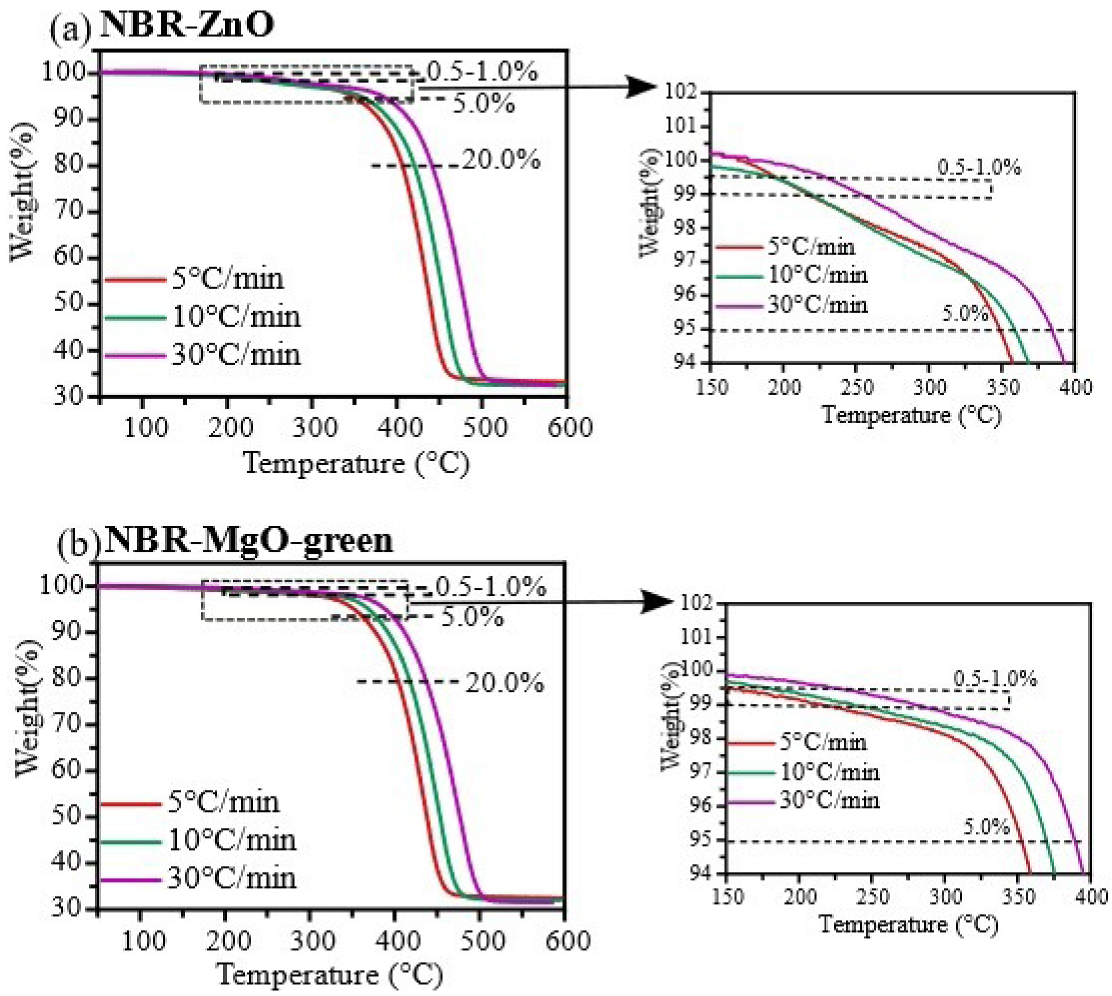

Figure 2. TGA at different heating rates of (a) NBR-ZnO; (b) NBR-MgO-green.

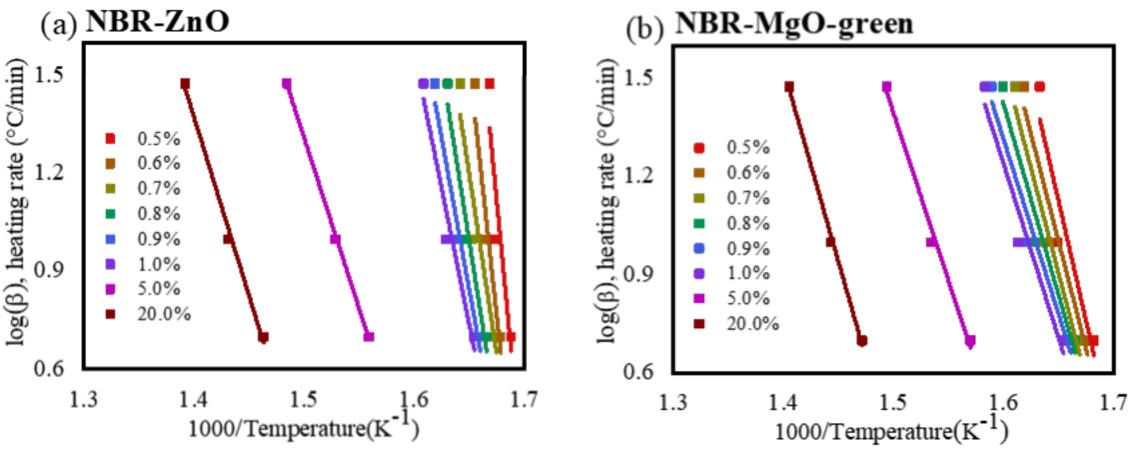

Figure 3. Ln (β) variation as a function of 1/T for composite with: (a) NBR-ZnO and (b) NBR- MgO-green.

previous hypothesis. Ren et al.[31] investigated the effect of conventional (CV), semi-efficient (SEV), and efficient (EV) system curing on the thermal degradation of sulfur-cured natural rubber using the Flynn-Wall-Ozawa method for

Table 2. Activation energy (E_a) by Flynn–Wall–Ozawa method.

Weight loss (wt%)	NBR-ZnO		NBR-MgO-green	
	E_a (kJ/mol)	R^2	E_a (kJ/mol)	R^2
0.5	700	0.8314	272	0.8910
0.6	614	0.8786	242	0.9404
0.7	427	0.8975	237	0.9463
0.8	411	0.9430	215	0.9647
0.9	352	0.9493	196	0.9660
1	309	0.9623	194	0.9551
5	194	0.9991	205	0.9997
20	211	0.9954	215	0.9969

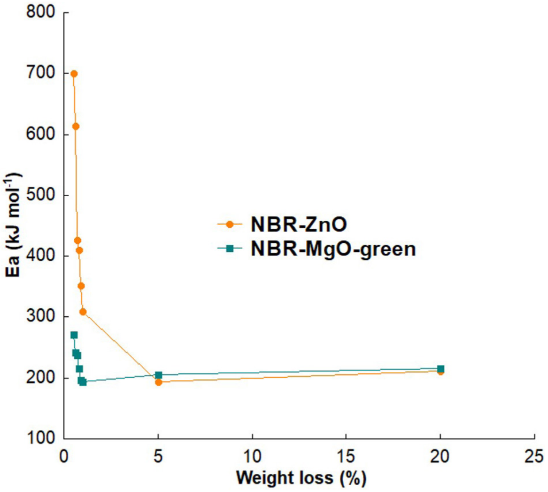

Figure 4. Activation energy (E_a) behavior for NBR-ZnO and NBR-MgO-green.

conversion rates ranging from 5 to 40%. According to the authors, the Ea increases in the following order CV > SEV > EV. Given that the CV system is used in this study, and based on Ren et al.'s results[31], the higher activation energy of NBR-ZnO compared to NBR-MgO-green by only 0.5 to 1%wt (Figure 4) can be attributed to the presence of defects in the network, and the amount of polysulfide linkages in NBR-MgO-green may be slightly higher than in NBR-ZnO.

3.2 Thermal-oxidative aging

Thermal-oxidative aging study is an essential test for assessing and comparing materials designed for industrial applications. Exposure of rubber material to oxidative thermal aging often results in changes in cross-links densities and mechanical properties. An increase in cross-link density leads to higher hardness and a decrease in final elongation[32-35]. The cross-links densities of NBR-ZnO and NBR-MgO-green before (B) and after (A) thermal-oxidative aging in a forced-air oven at 100 °C for 72 h are shown in Table 3. Prior to thermal aging, NBR-MgO-green has a slightly higher cross-link density than NBR-ZnO. After oxidative-thermal aging, the crosslink density of NBR-ZnO increased and surpassed that of NBR-MgO-green. This result suggests the occurrence of extra cross-linking in both samples, but with greater intensity in NBR-ZnO.

Table 3. Cross-link Density of NBR composites before (B) and after (A) aging.

Composite	Crosslink Density (mol cm^{-3})
NBR-ZnO (B)	3.8E-04
NBR-ZnO (A)	8.4E-04
NBR-MgO-green (B)	5.9E-04
NBR-MgO-green (A)	7.3E-04

Figure 5 shows the mean plot of hardness Shore A, stress at 100% of strain, tensile strength, and ultimate elongation of NBR-ZnO and NBR-MgO-green before and after thermal-oxidative aging. The intervals of mean of mechanical properties were calculated based on Fisher's least significant difference (LSD) procedure[36]. In this method, if two means are the same, their intervals will overlap 95.0% of the time.

For example, Han et al.[33] studied thermo-oxidative aging in NBR composites through cross-link density and mechanical properties. Thermal oxidative aging was carried out with aging at 125, 135, and 150 °C and aging time of 10, 22, 34, 46, 58, and 70 h. The crosslink density increased as the temperature and heating time increased, associated with oxidative cross-linking reactions of unsaturated bonds in the NBR molecular chains. Tensile strength gradually decreased[33].

Hardness increased after thermal aging in line with the cross-link density, observed in Figure 5a, with a more significant increase in the NBR-ZnO composite. The stress at 100% strain before aging the compositions had similar values and after aging it increased for both compositions in agreement with the increase in cross-links also after aging. And this increase in tension at 100% strain is greater for NBR-ZnO, observed in Figure 5b, as it presented higher values in the crosslinking network with aging, as shown in Table 3. The Tensile strength before heating presented similar values for the compositions, after aging the influence of cross-link density also influenced the increase in the value for the NBR-ZnO composite. The increase in cross-link density also had an effect on the ultimate elongation, decreasing the values in both compositions after aging (Figure 5d). Overall NBR composition with ZnO and MgO-green exhibited good aging resistance. The NBR-MgO were

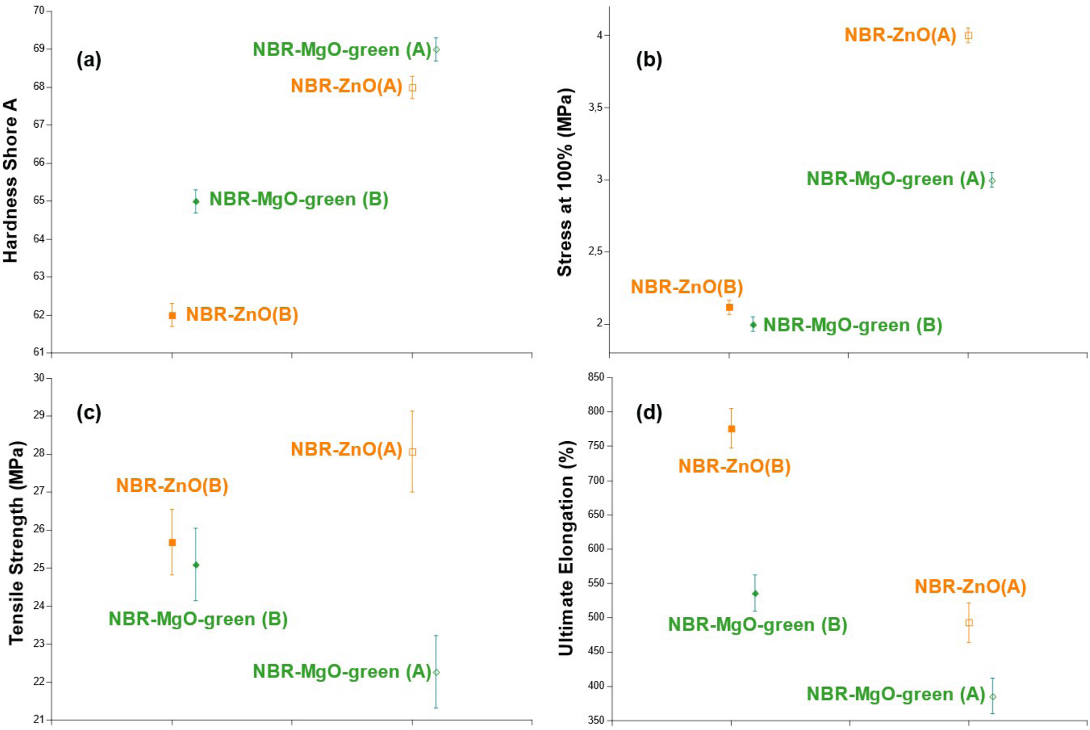

Figure 5. Mechanical properties before (B) and after (A) Thermal Aging: (a) Shore A Hardness, (b) Stress at 100% of Strain, (c) Tensile Strength, and (d) Ultimate Elongation.

less sensitive to changes when compared to the difference in property values after thermal aging. This sensitivity of the NBR-ZnO composites is related to the fact that the difference in cross-link density after and before ageing is much greater than for the NBR-MgO-green compositions.

4. Conclusions

The possibility of replacing the current ZnO activator in the vulcanization system with green-MgO synthesized by a more ecologically viable route was investigated in this study, focusing on thermal behavior. The conclusion was that MgO-green is a promising and valuable activator to replace ZnO. A lower sensitivity with thermal aging when compared to ZnO showed a potential improvement in the thermal stability of the MgO-green, especially in general in the mechanical properties based on Fisher's least significant difference (LSD) procedure.

5. Author's Contribution

- **Conceptualization** – Ana Maria Furtado de Sousa; Nakédia Maysa Freitas Carvalho.
- **Data curation** – Arianne Aparecida da Silva.
- **Formal analysis** – Arianne Aparecida da Silva.
- **Funding acquisition -** Ana Maria Furtado de Sousa; Nakédia Maysa Freitas Carvalho.
- **Investigation** – Arianne Aparecida da Silva.
- **Methodology** – NA.
- **Project administration** – Cristina Russi Guimarães Furtado.
- **Resources** – Ana Maria Furtado de Sousa; Nakédia Maysa Freitas Carvalho.
- **Software –** NA.
- **Supervision –** Cristina Russi Guimarães Furtado**.**
- **Validation –** NA.
- **Visualization** – NA.
- **Writing – original draft –** Arianne Aparecida da Silva.
- **Writing – review & editing –** Ana Maria Furtado de Sousa; Nakédia Maysa Freitas Carvalho; Cristina Russi Guimarães Furtado.

6. Acknowledgements

The authors thank Nitriflex for donating the raw materials and for the use of its facilities. This study was supported by the CAPES) [Financing code 001,: PhD Scholarship received by Arianne A. da Silva]; Conselho Nacional de Desenvolvimento Científico e Tecnológico (CNPQ) [P2-309461/2021-9 received by Ana Maria Furtado de Sousa and PQ-2/2021: 316550/2021–3 received by Nakédia M. F. Carvalho] and Fundação Carlos Chagas Filho de Amparo à Pesquisa do Estado do Rio de Janeiro – FAPERJ [CNE 2021: E-26/200.416/2023 and Grupos Emergentes 2019: E-26/010.002171/2019 received by Nakédia M. F. Carvalho; APQ1 2019:

E-26/010.001927/2019 received by Ana Maria Furtado de Sousa.

7. References

1. Lou, W., Zhang, W., Wang, H., Jin, T., & Liu, X. (2018). Influence of hydraulic oil on degradation behavior of nitrile rubber O-rings at elevated temperature. *Engineering Failure Analysis*, *92*, 1-11. http://doi.org/10.1016/j.engfailanal.2018.05.006.
2. Wei, X., Wu, H., Zhang, L., Zhang, S.-y., Xiao, Y., & Luo, T.-y. (2018). Failure analysis of nitrile rubber o-rings static sealing for packaging barrel. *Journal of Failure Analysis and Prevention*, *18*(3), 628-634. http://doi.org/10.1007/s11668-018-0451-3.
3. Chopra, A., & Singh, S. (2022). Major application and impact after modified bituminous with nitrile rubber and thermoset: an analysis. *Materials Today: Proceedings*, *51*(Pt 1), 977-987. http://doi.org/10.1016/j.matpr.2021.07.021.
4. Ghamarpoor, R., & Jamshidi, M. (2022). Preparation of superhydrophobic/superoleophilic nitrile rubber (NBR) nanocomposites contained silanized nano silica for efficient oil/water separation. *Separation and Purification Technology*, *291*, 120854. http://doi.org/10.1016/j.seppur.2022.120854.
5. Zou, Y., Sun, Y., He, J., Tang, Z., Zhu, L., Luo, Y., & Liu, F. (2016). Enhancing mechanical properties of styrene–butadiene rubber/silica nanocomposites by in situ interfacial modification with a novel rare-earth complex. *Composites. Part A, Applied Science and Manufacturing*, *87*, 297-309. http://doi.org/10.1016/j.compositesa.2016.05.006.
6. Mostoni, S., Milana, P., Di Credico, B., D'Arienzo, M., & Scotti, R. (2019). Zinc-based curing activators: new trends for reducing zinc content in rubber vulcanization process. *Catalysts*, *9*(8), 664. http://doi.org/10.3390/catal9080664.
7. Roy, K., Alam, M. N., Mandal, S. K., & Debnath, S. C. (2015). Preparation of zinc-oxide-free natural rubber nanocomposites using nanostructured magnesium oxide as cure activator. *Journal of Applied Polymer Science*, *132*(43), app.42705. http://doi.org/10.1002/app.42705.
8. Zanchet, A., Sousa, F. D. B., Crespo, J. S., & Scuracchio, C. H. (2018). Activator from sugar cane as a green alternative to conventional vulcanization additives. *Journal of Cleaner Production*, *174*, 437-446. http://doi.org/10.1016/j.jclepro.2017.10.329.
9. Silva, A. A., Rocha, E. B. D., Furtado, C. R. G., Sousa, A. M. F., & Carvalho, N. M. F. (2021). Magnesium oxide biosynthesized with *Camellia sinensis* extract as activator in nitrile rubber vulcanization. *Polymer Bulletin*, *78*(11), 6205-6219. http://doi.org/10.1007/s00289-020-03430-x.
10. Przybyszewska, M., Zaborski, M., Jakubowski, B., & Zawadiak, J. (2009). Zinc chelates as new activators for sulphur vulcanization of acrylonitrile-butadiene elastomer. *Express Polymer Letters*, *3*(4), 256-266. http://doi.org/10.3144/expresspolymlett.2009.32.
11. Heideman, G., Noordermeer, J. W. M., Datta, R. N., & Van Baarle, B. (2003). Modified clays as activator in sulphur vulcanisation: A novel approach to reduce zinc oxide levels in rubber compounds. *Kautschuk und Gummi, Kunststoffe*, *56*(12), 650.
12. Heideman, G., Noordermeer, J. W. M., Datta, R. N., & Van Baarle, B. (2004). Zinc loaded clay as activator in sulfur vulcanization: a new route for zinc oxide reduction in rubber compounds. *Rubber Chemistry and Technology*, *77*(2), 336-355. http://doi.org/10.5254/1.3547827.
13. Moresco, S., Giovanela, M., Carli, L. N., & Crespo, J. S. (2016). Development of passenger tire treads: reduction in zinc content and utilization of a bio-based lubricant. *Journal of Cleaner Production*, *117*, 199-206. http://doi.org/10.1016/j.jclepro.2016.01.013.
14. Zanchet, A., Demori, R., Sousa, F. D. B., Ornaghi, H. L., Jr., Schiavo, L. S. A., & Scuracchio, C. H. (2019). Sugar cane as an alternative green activator to conventional vulcanization additives in natural rubber compounds: thermal degradation study. *Journal of Cleaner Production*, *207*, 248-260. http://doi.org/10.1016/j.jclepro.2018.09.203.
15. Alam, M. N., Kumar, V., & Park, S.-S. (2022). Advances in rubber compounds using ZnO and MgO as co-cure activators. *Polymers*, *14*(23), 5289. http://doi.org/10.3390/polym14235289. PMid:36501682.
16. Silva, A. A., Rocha, E. B. D., Linhares, F. N., Sousa, A. M. F., Carvalho, N. M., & Furtado, C. R. G. (2022). Replacement of ZnO by ecofriendly synthesized MgO in the NBR vulcanization. *Polymer Bulletin*, *79*(10), 8535-8549. http://doi.org/10.1007/s00289-021-03921-5.
17. Pilarska, A. A., Klapiszewski, Ł., & Jesionowski, T. (2017). Recent development in the synthesis, modification and application of $Mg(OH)_2$ and MgO: A review. *Powder Technology*, *319*, 373-407. http://doi.org/10.1016/j.powtec.2017.07.009.
18. Hornak, J., Trnka, P., Kadlec, P., Michal, O., Mentlík, V., Šutta, P., Csányi, G. M., & Tamus, Z. Á. (2018). Magnesium oxide nanoparticles: dielectric properties, surface functionalization and improvement of epoxy-based composites insulating properties. *Nanomaterials (Basel, Switzerland)*, *8*(6), 381. http://doi.org/10.3390/nano8060381. PMid:29848967.
19. Flynn, J. H., & Wall, L. A. (1966). A quick, direct method for the determination of activation energy from thermogravimetric data. *Journal of Polymer Science. Part B: Polymer Letters*, *4*(5), 323-326. http://doi.org/10.1002/pol.1966.110040504.
20. Rajeshwari, P. (2016). Kinetic analysis of the non-isothermal degradation of high-density polyethylene filled with multi-wall carbon nanotubes. *Journal of Thermal Analysis and Calorimetry*, *123*(2), 1523-1544. http://doi.org/10.1007/s10973-015-5021-2.
21. Erbetta, C. D. C., Azevedo, R. C. S., Andrade, K. S., Silva, M. E. S. R., Freitas, R. F. S., & Sousa, R. G. (2017). Characterization and lifetime estimation of high density polyethylene containing a prodegradant agent. *Materials Sciences and Applications*, *8*(13), 979-991. http://doi.org/10.4236/msa.2017.813072.
22. Shuhaimi, N. H. H., Ishak, N. S., Othman, N., Ismail, H., & Sasidharan, S. (2014). Effect of different types of vulcanization systems on the mechanical properties of natural rubber vulcanizates in the presence of oil palm leaves-based antioxidant. *Journal of Elastomers and Plastics*, *46*(8), 747-764. http://doi.org/10.1177/0095244313489910.
23. Sun, J., Wang, X., & Zong, C. (2020). Evaluation of hot air degradation activation energy of carbon black filled hydrogenated nitrile butadiene rubber using Flynn-Wall-Ozawa approach. *IOP Conference Series: Earth and Environmental Science*, *514*, 052002. http://doi.org/10.1088/1755-1315/514/5/052002.
24. Zhang, J., Li, J., Liu, M., Zhao, Y., & Wang, S. (2016). Thermal decomposition kinetics and mechanism of low-temperature hydrogenated acrylonitrile butadiene rubber composites with sodium methacrylate. *Chemical Research in Chinese Universities*, *32*(6), 1045-1051. http://doi.org/10.1007/s40242-016-6148-9.
25. Hwang, W.-G., Wei, K.-H., & Wu, C.-M. (2004). Mechanical, thermal, and barrier properties of NBR/organosilicate nanocomposites. *Polymer Engineering and Science*, *44*(11), 2117-2124. http://doi.org/10.1002/pen.20217.
26. Oliveira, I. T., Pacheco, É. B. A. V., Visconte, L. L. Y., Oliveira, M. R., & Rubinger, M. M. M. (2010). Effect of a new accelerator of vulcanization in the rheometric properties of nitrile rubber compositions with different AN amounts. *Polímeros: Ciência e Tecnologia*, *20*(5), 366-370. http://doi.org/10.1590/S0104-14282010005000059.
27. Lee, Y. S., & Ha, K. (2021). Effects of acrylonitrile content on thermal characteristics and thermal aging properties of carbon

black-filled NBR composite. *Journal of Elastomers and Plastics*, *53*(5), 402-416. http://doi.org/10.1177/0095244320941243.

28. Hong, I. K., & Lee, S. (2013). Cure kinetics and modeling the reaction of silicone rubber. *Journal of Industrial and Engineering Chemistry*, *19*(1), 42-47. http://doi.org/10.1016/j.jiec.2012.05.006.
29. Plota, A., & Masek, A. (2020). Lifetime prediction methods for degradable polymeric materials—A short review. *Materials*, *13*(20), 4507. http://doi.org/10.3390/ma13204507
30. Liu, S., Yu, J., Bikane, K., Chen, T., Ma, C., Wang, B., & Sun, L. (2018). Rubber pyrolysis: kinetic modeling and vulcanization effects. *Energy*, *155*, 215-225. http://doi.org/10.1016/j.energy.2018.04.146.
31. Ren, T., Wan, C., Song, P., Rodrigue, D., Zhang, Y., & Wang, S. (2024). Thermo-oxidative degradation behavior of natural rubber vulcanized by different curing systems. *Chemical Engineering Science*, *295*, 120147. http://doi.org/10.1016/j.ces.2024.120147.
32. Krishnamurthy, S., & Balakrishnan, P. (2019). Dynamic mechanical behavior, solvent resistance and thermal degradation of nitrile rubber composites with carbon black-halloysite nanotube hybrid fillers. *Polymer Composites*, *40*(S2), E1612-E1621. http://doi.org/10.1002/pc.25101.
33. Han, R., Wu, Y., Quan, X., & Niu, K. (2020). Effects of crosslinking densities on mechanical properties of nitrile rubber composites in thermal oxidative aging environment. *Journal of Applied Polymer Science*, *137*(36), 49076. http://doi.org/10.1002/app.49076.
34. Mengistu, T., & Pazur, R. J. (2021). The thermal oxidation of hydrogenated acrylonitrile-co-butadiene rubber from ambient to 150°C. *Polymer Degradation & Stability*, *188*, 109574. http://doi.org/10.1016/j.polymdegradstab.2021.109574.
35. Senthilvel, K., Pasupathy, J., Kumar, A. A. J., Rathinam, N., & Prabu, B. (2022). Investigation on the ageing properties of nitrile rubber reinforced halloysite nanotubes/carbon black hybrid composites. *Materials Today: Proceedings*, *68*(Pt 6), 2665-2675. http://doi.org/10.1016/j.matpr.2022.09.559.
36. Meier, U. (2006). A note on the power of Fisher's least significant difference procedure. *Pharmaceutical Statistics: The Journal of Applied Statistics in the Pharmaceutical Industry*, *5*(4), 253-263. http://doi.org/10.1002/pst.210. PMid:17128424.

Received: Aug. 19, 2024
Revised: Dec. 03, 2024
Accepted: Dec. 17, 2024